JOURNAL OF SOLID STATE CHEMISTRY 69, 67–75 (1987)

Structure Determination of Low-Dimensional Conductor Sodium Molybdenum Purple Bronze $Na_{0.9}Mo_6O_{17}$

M. ONODA,* Y. MATSUDA, AND M. SATO

Institute for Molecular Science, Okazaki National Research Institutes, Myodaiji, Okazaki 444, Japan

Received June 30, 1986; in revised form October 22, 1986

Structure determination of the molybdenum purple bronze $Na_{0.9}Mo_6O_{17}$ is carried out by single-crystal X-ray diffraction. The crystal is monoclinic with space group $A2$ and the lattice constants are a = 12.983(2), b = 5.518(1), c = 9.591(2) Å, β = 89.94(1)°, Z = 2. Full-matrix least-squares refinement gives the final values of R(F) = 0.028 and R_w(F) = 0.040 for 1484 independent reflections, in which the occupancy factor of the sodium atom becomes 0.899(12). The present structure is built up of the linkage of the MoO_4 and MoO_6 polyhedra. There are slabs which consist of four layers of distorted MoO_6 octahedra sharing corners. Both the structure and the molybdenum valence distribution estimated from the Mo–O bond lengths are considered to lead to the two-dimensional electronic transport. This structure is compared with those of other members of molybdenum purple bronzes, $K_{0.9}Mo_6O_{17}$ and $Li_{0.9}Mo_6O_{17}$. The difference of the electronic properties among these compounds can be well understood on the basis of their structural characteristics.

Introduction

Transition metal bronzes M_xTO_n, where T is a transition metal atom and M is an alkali metal atom, etc., have various interesting physical properties which arise from their charateristic crystal structures. The electrons donated into the TO_n cage band by the M atom contribute to the electrical conduction. With respect to the electronic natures, there are two extreme groups depending on the species of the T atoms. One includes the compounds with wide-band metallic electrons; for example, many of the tungsten bronzes M_xWO_3 are good conductors and often become superconducting (*1*). The other includes the compounds with narrow-band localized electrons; for example, the vanadium bronzes $M_xV_2O_5$ have the phase transitions to the insulating states, or a kind of the charge-density-wave (CDW) states due to the strong electron–phonon interaction (*2*).

The molybdenum bronzes M_xMoO_n are considered to be located near the metal–insulator boundary and even the small anisotropy of the structure induces the low-dimensional conducting properties, which have been a subject of extensive studies (*3*). A metal–insulator transition in the molybdenum blue bronzes $M_{0.3}MoO_3$ (M = K, Rb, and Tl) has been studied from the viewpoint of the CDW motion.

The molybdenum purple bronzes $M_{0.9}Mo_6O_{17}$ (M = Li, Na, and K) are another series of molybdenum bronzes (*4–6*). In this case, there are not only the conduction electrons donated by the M atoms but also

* To whom correspondence should be addressed.

0022-4596/87 $3.00

the lack of oxygen atoms compared with the highest class oxide MoO_3. The compound $K_{0.9}Mo_6O_{17}$ is a two-dimensional conductor and undergoes the phase transition to the CDW state at about 105 K, where the wave vector of the structural modulation is (0.5, 0.5, 0) in reciprocal space (*7, 8*). A similar CDW transition has also been observed in $Na_{0.9}Mo_6O_{17}$ at about 70 K (*9, 10*), which implies that both compounds have similar electronic properties. On the other hand, $Li_{0.9}Mo_6O_{17}$, whose conduction is anisotropic even in the cleavage plane, exhibits superconductivity below about 2 K after the rapid upturn of the resistivity with decreasing temperature (*11*). The interesting problems of the superconductivity–CDW competition in these compounds and of the origin of the anomalous temperature dependence of the resistivity in $Li_{0.9}Mo_6O_{17}$ have been noted. In order to investigate these problems, detailed information about the crystal structures of the present series of compounds is necessary. Up to now, the structures of $K_{0.9}Mo_6O_{17}$ and $Li_{0.9}Mo_6O_{17}$ have been determined by Vincent *et al.* (*12*) and the present authors (*13*), respectively. The conduction electron distributions have also been estimated based on the observed Mo–O bond lengths. The structural properties of $K_{0.9}Mo_6O_{17}$ and $Li_{0.9}Mo_6O_{17}$ have successfully explained the large anisotropies of the resistivities found in these compounds. Although the structure of $Na_{0.9}Mo_6O_{17}$ was partially solved by Stephenson (*14*) for twinned crystal, no precise atomic coordinates or bond lengths have been published.

On the basis of the above background, the structure determination of $Na_{0.9}Mo_6O_{17}$ was carried out by single-crystal X-ray diffraction. Here one can expect that the structure of $N_{0.9}Mo_6O_{17}$ is not so different from that of $K_{0.9}Mo_6O_{17}$, since the electronic properties of both crystals are similar as was mentioned above. In the next section, the experimental technique and the refinement procedure are presented. In the third section, the crystal structure of $Na_{0.9}Mo_6O_{17}$ is described and the effective mean molybdenum valences are estimated based on the observed Mo–O bond lengths. The problem of the superconductivity–CDW competition in the molybdenum purple bronzes is also discussed relative to their structural properties. The last section is devoted to a conclusion.

Experiment and Refinement

Purple-colored single crystals of $Na_{0.9}Mo_6O_{17}$ with platelet shape were prepared by electrolysis as described by Wold *et al.* (*4*). Intensity data were collected at room temperature on a Rigaku AFC-5R four-circle diffractometer with graphite-monochromatized MoK_α radiation, employing the θ–2θ scan technique. A crystal of dimensions 0.03 × 0.21 × 0.22 mm, along the ⟨100⟩, ⟨011⟩, and ⟨01$\bar{3}$⟩ directions, respectively, was used for the data collection up to $2\theta = 70°$. Of the total number of 3366 reflections, 1608 independent reflections with $|F_o| > 3\sigma(|F_o|)$ were obtained and used for the structure analysis, where the reflection number with $|F_o| < 3\sigma(|F_o|)$ was 54. Lorentz-polarization and absorption corrections were applied. The minimal and maximal transmission factors were 0.356 and 0.843, respectively. The internal R value was $R_{int} = 0.010$. The unit cell dimensions were determined by a least-squares calculation based on forty 2θ values ($25° \leq 2\theta \leq 30°$). The crystal data are summarized in Table I with those of $K_{0.9}Mo_6O_{17}$ (*12*) and $Li_{0.9}Mo_6O_{17}$ (*13*).

The structure was solved from three-dimensional Patterson maps calculated by the Universal Crystallographic Computation Program System UNICS III (*15*) and refined by the full-matrix least-squares program RADIEL (*16*). Here an isotropic secondary extinction effect was assumed, its

value being 4.50×10^{-4}. The weighting factor, $w = [\sigma(\text{counting statistics})^2 + (0.010\,|F_o|)^2]^{-1}$, was employed. The sodium and oxygen atom positions were derived from difference Fourier maps. The refinement with the space group $A2$ and with the isotropic temperature factors for all the atoms gave $R = \Sigma||F_o| - |F_c||/\Sigma|F_o| = 0.037$ and $R_w = \{[\Sigma\, w(|F_o| - |F_c|)^2]/\Sigma\, w|F_o|^2\}^{1/2} = 0.058$. The introduction of the anisotropic temperature factors gave $R = 0.030$ and $R_w = 0.050$. In the subsequent calculations, the 124 low-angle reflections with the extinction factors less than 0.9 were omitted in order to improve the accuracy of the atomic parameters. The final refinement was carried out for 1484 reflections, leading to the values of $R = 0.028$ and $R_w = 0.040$. In this refinement, the occupancy factor of the sodium atom was found to be 0.899(12). Other possible space groups $A2/m$ and Am, expected from the Laue group $A2/m$, should be excluded because of the large R and R_w and the abnormal temperature factors. The atomic scattering factors and the anomalous-scattering corrections were taken from "International Tables for X-Ray Crystallography" (*17*). A table of the observed and calculated structure factors has been deposited with the National Auxiliary Publications Service.[1] The calculations were carried out on the HITAC M-680H computer at the Computer Center of the Institute for Molecular Science.

[1] See NAPS document No. 04452 for 10 pages of supplementary material. Order from ASIS/NAPS, Microfiche Publications, P.O. Box 3513, Grand Central Station, New York, NY 10163. Remit in advance $4.00 for microfiche copy or for photocopy, $7.75 up to 20 pages plus $.30 for each additional page. All orders must be prepaid. Institutions and organizations may order by purchase order. However, there is a billing and handling charge for this service of $15. Foreign orders add $4.50 for postage and handling, for the first 20 pages, and $1.00 for additional 10 pages of material, $1.50 for postage of any microfiche orders.

TABLE I

CRYSTAL DATA OF MOLYBDENUM PURPLE BRONZES

	$K_{0.9}Mo_6O_{17}$[a]	$Na_{0.9}Mo_6O_{17}$[b]	$Li_{0.9}Mo_6O_{17}$[c]
System	Trigonal	Monoclinic	Monoclinic
Space group	$P\bar{3}$	$A2$	$P2_1/m$
Z	1	2	2
a (Å)	5.538(1)	12.983(2)	12.762(2)
b (Å)		5.518(1)	5.523(1)
c (Å)	13.656(2)	9.591(2)	9.499(1)
β (°)		89.94(1)	90.61(1)
V (Å^3)	362.7	687.1(2)	669.5(1)
μ (MoK_α)(mm^{-1})	5.26	5.32	5.43
D_x (Mg m^{-3})	4.04	4.20	4.24

[a] Ref. (*12*).
[b] Present work.
[c] Ref. (*13*).

Results and Discussion

(a) *Description of the Structure*

The positional parameters and the equivalent isotropic thermal parameters of the atoms are listed in Table II, and the anisotropic thermal parameters are in Table III. The selected interatomic distances and angles are presented in Table IV. The crystal

TABLE II

ATOMIC COORDINATES ($\times 10^5$) AND EQUIVALENT ISOTROPIC THERMAL PARAMETERS (Å^2)

Atom		x	y	z	B_{eq}[a]
Mo(1)	4*c*	7480(3)	1729(13)	33344(3)	0.43(1)
Mo(2)	4*c*	23141(3)	2064(12)	9(3)	0.40(1)
Mo(3)	4*c*	38666(3)	0	66694(3)	0.48(1)
Na[b]	2*b*	50000	47382(103)	50000	2.01(9)
O(1)	2*a*	0	941(131)	50000	0.78(9)
O(2)	4*c*	16707(32)	3378(98)	16497(31)	1.11(8)
O(3)	4*c*	34399(30)	49619(120)	34240(30)	1.40(8)
O(4)	4*c*	48286(32)	3877(80)	33638(48)	1.95(9)
O(5)	4*c*	591(49)	25751(89)	75096(57)	0.68(6)
O(6)	4*c*	16009(42)	28694(80)	41846(50)	1.12(8)
O(7)	4*c*	17436(38)	27726(84)	91762(48)	0.93(8)
O(8)	4*c*	33118(48)	24911(98)	57933(51)	1.56(11)
O(9)	4*c*	35363(41)	22557(85)	7745(52)	1.11(8)

[a] $B_{eq} = \frac{4}{3}\sum_i\sum_j \beta_{ij}\mathbf{a}_i \cdot \mathbf{a}_j$, where β_{ij} ($i, j = 1, 2$, and 3) are defined by the equation $\exp[-(\beta_{11}h^2 + \beta_{22}k^2 + \beta_{33}l^2 + 2\beta_{12}hk + 2\beta_{13}hl + 2\beta_{23}kl)]$.
[b] Occupancy probability = 89.9(1.2)%.

TABLE III

ANISOTROPIC THERMAL PARAMETERS ($\times 10^4$)[a]

Atom	U_{11}	U_{22}	U_{33}	U_{12}	U_{13}	U_{23}
Mo(1)	60(2)	56(2)	46(1)	0(1)	0(1)	0(1)
Mo(2)	48(2)	45(2)	60(1)	−3(1)	0(1)	−1(1)
Mo(3)	60(2)	73(2)	50(1)	0(2)	0(1)	0(1)
Na	105(15)	284(21)	374(20)		−13(13)	
O(1)	138(20)	112(22)	48(14)		−6(13)	
O(2)	146(15)	140(20)	137(14)	−9(17)	89(12)	5(13)
O(3)	241(20)	191(20)	100(12)	13(22)	93(12)	−3(16)
O(4)	90(16)	179(21)	471(23)	47(17)	5(16)	47(19)
O(5)	86(15)	102(15)	71(10)	−17(13)	−17(9)	−23(11)
O(6)	140(20)	73(16)	213(19)	−30(15)	−70(16)	−26(14)
O(7)	104(19)	91(16)	158(16)	43(15)	−26(14)	26(13)
O(8)	307(31)	177(20)	100(16)	116(21)	−14(17)	22(14)
O(9)	123(19)	133(17)	166(17)	−19(16)	−55(14)	−24(14)

[a] $U_{ij} = \beta_{ij}/2\pi^2 \mathbf{a}_i^* \cdot \mathbf{a}_j^*$.

structure projected on the *ac*-plane is shown in Fig. 1 with the atom-numbering scheme. For comparison, the crystal structures of $K_{0.9}Mo_6O_{17}$ (*12*) and $Li_{0.9}Mo_6O_{17}$ (*13*) are also shown in Figs. 2 and 3, respectively. The unit cell of $Na_{0.9}Mo_6O_{17}$ contains three crystallographically independent molybdenum atoms, labelled Mo(1), Mo(2), and Mo(3). The Mo(1) and Mo(2) atoms are located in the oxygen octahedra, while the Mo(3) atom is inside the oxygen tetrahedra. The present structure is found to be built up of slabs of the MoO_6 octahedra connected with the MoO_4 tetrahedra. Each slab has four layers of distorted ReO_3-type MoO_6 octahedra sharing corners, parallel to the *bc*-plane. The sodium atoms are located in the large vacant sites between the slabs and they are within the oxygen icosahedra linked to the $Mo(3)O_4$ tetrahedra as shown in Fig. 4. The Na–O distances listed in Table IV are in the usual range.

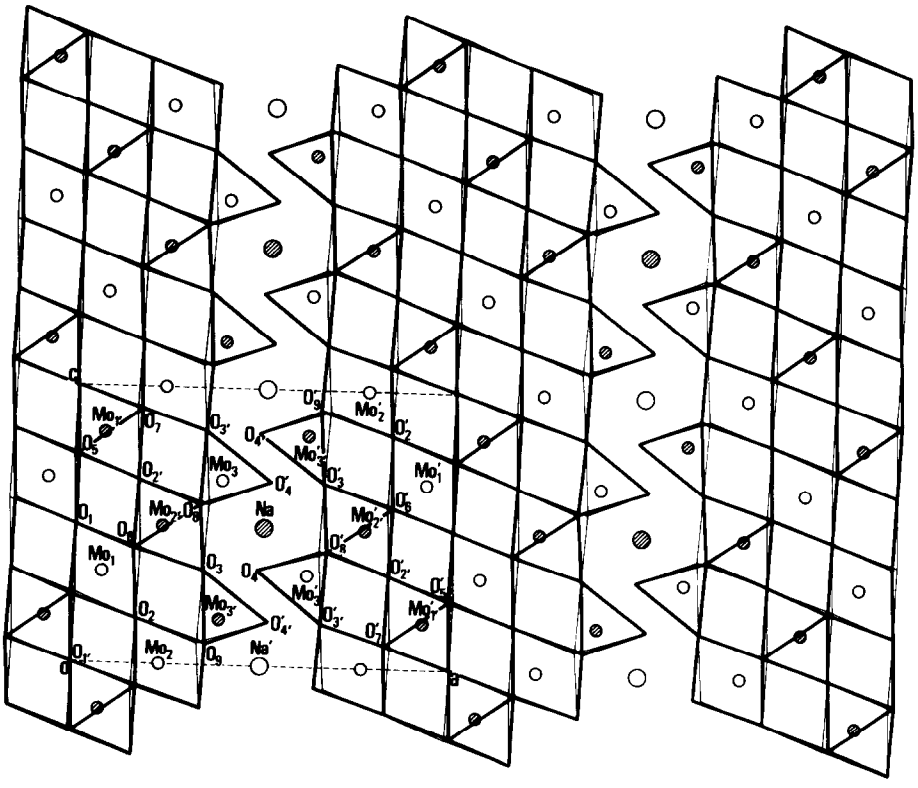

FIG. 1. Crystal structure of $Na_{0.9}Mo_6O_{17}$ projected on the *ac*-plane. Open and hatched circles indicate atomic positions at $y \simeq 0$ and $\frac{1}{2}$, respectively.

TABLE IV

SELECTED INTERATOMIC DISTANCE (Å) AND ANGLES (°)

Mo(1) octahedron			
Mo(1)–O(1)	1.869(0)	O(1)–Mo(1)–O(7)[a]	88.58(14)
Mo(1)–O(2)	2.012(3)	O(2)–Mo(1)–O(5)[a]	88.83(19)
Mo(1)–O(5)[a]	1.866(5)	O(2)–Mo(1)–O(5)[b]	87.35(20)
Mo(1)–O(5)[b]	1.874(6)	O(2)–Mo(1)–O(6)	87.98(17)
Mo(1)–O(6)	2.027(5)	O(2)–Mo(1)–O(7)[a]	88.28(17)
Mo(1)–O(7)[a]	2.020(3)	O(5)[a]–Mo(1)–O(5)[b]	95.27(24)
		O(5)[a]–Mo(1)–O(6)	175.52(22)
O(1)–Mo(1)–O(2)	174.59(10)	O(5)[a]–Mo(1)–O(7)[a]	88.45(22)
O(1)–Mo(1)–O(5)[a]	95.49(17)	O(5)[b]–Mo(1)–O(6)	87.74(22)
O(1)–Mo(1)–O(5)[b]	95.47(17)	O(5)[b]–Mo(1)–O(7)[a]	174.21(22)
O(1)–Mo(1)–O(6)	87.52(14)	O(6)–Mo(1)–O(7)[a]	88.31(19)
Mo(2) octahedron			
Mo(2)–O(2)	1.789(3)	O(2)–Mo(2)–O(9)	91.05(18)
Mo(2)–O(3)[a]	2.106(3)	O(3)[a]–Mo(2)–O(6)[a]	89.92(18)
Mo(2)–O(6)[a]	1.771(5)	O(3)[a]–Mo(2)–O(7)[c]	91.18(18)
Mo(2)–O(7)[c]	1.783(5)	O(3)[a]–Mo(2)–O(8)[a]	77.79(18)
Mo(2)–O(8)[a]	2.122(6)	O(3)[a]–Mo(2)–O(9)	76.26(17)
Mo(2)–O(9)	2.086(5)	O(6)[a]–Mo(2)–O(7)[c]	99.47(22)
		O(6)[a]–Mo(2)–O(8)[a]	87.93(22)
O(2)–Mo(2)–O(3)[a]	163.77(14)	O(6)[a]–Mo(2)–O(9)	161.93(21)
O(2)–Mo(2)–O(6)[a]	100.16(19)	O(7)[c]–Mo(2)–O(8)[a]	166.77(22)
O(2)–Mo(2)–O(7)[c]	99.56(19)	O(7)[c]–Mo(2)–O(9)	92.51(21)
O(2)–Mo(2)–O(8)[a]	89.81(19)	O(8)[a]–Mo(2)–O(9)	77.91(21)
Mo(3) tetrahedron			
Mo(3)–O(3)[d]	1.771(3)	O(3)[d]–Mo(3)–O(8)	109.52(20)
Mo(3)–O(4)[e]	1.708(4)	O(3)[d]–Mo(3)–O(9)[d]	111.72(18)
Mo(3)–O(8)	1.765(5)	O(4)[e]–Mo(3)–O(8)	107.39(23)
Mo(3)–O(9)[d]	1.793(5)	O(4)[e]–Mo(3)–O(9)[d]	109.55(21)
		O(8)–Mo(3)–O(9)[d]	109.39(23)
O(3)[d]–Mo(3)–O(4)[e]	109.18(17)		
Na icosahedron			
Na–O(3)	2.532(4)	Na–O(4)[f]	3.253(5)
Na–O(4)	2.877(7)	Na–O(9)[f]	2.468(6)
Na–O(8)	2.630(7)		
Mo–Mo			
Mo(1)–Mo(1)[b]	3.737(1)	Mo(2)–Mo(3)[g]	3.691(1)
Mo(1)–Mo(2)	3.787(1)	Mo(2)–Mo(3)[c]	3.778(1)
Mo(1)–Mo(2)[f]	3.796(1)		

[a] $x, -\frac{1}{2} + y, -\frac{1}{2} + z$.
[b] $-x, y, 1 - z$.
[c] $x, y, -1 + z$.
[d] $x, -\frac{1}{2} + y, \frac{1}{2} + z$.
[e] $1 - x, y, 1 - z$.
[f] $x, \frac{1}{2} + y, \frac{1}{2} + z$.
[g] $x, \frac{1}{2} + y, -\frac{1}{2} + z$.

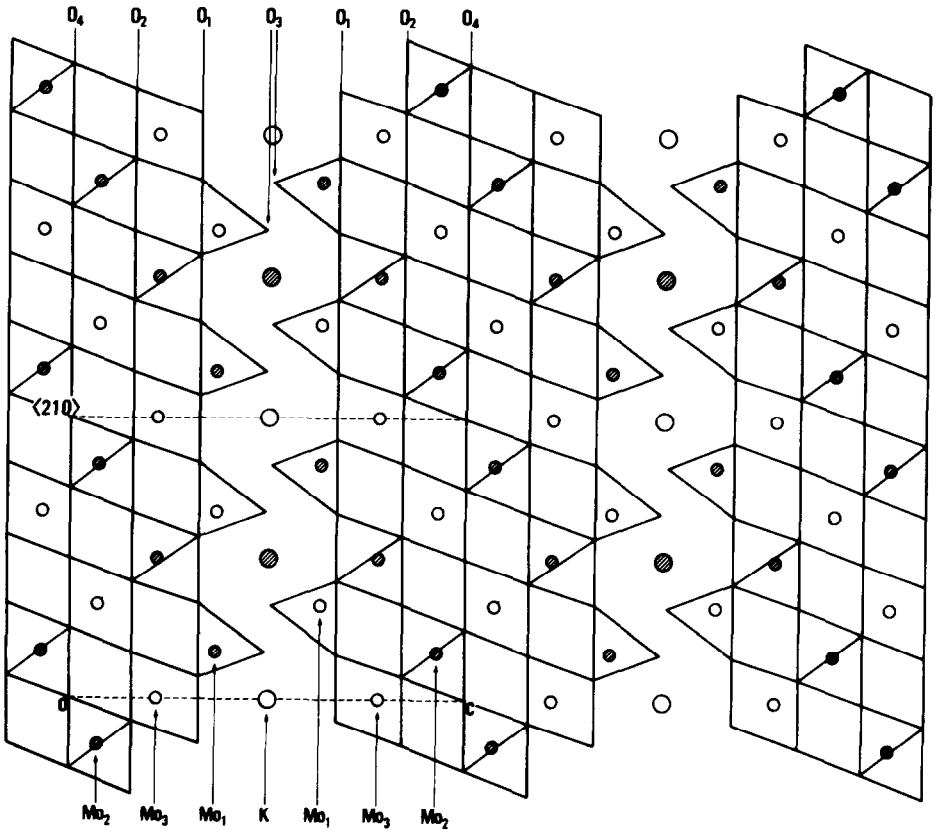

FIG. 2. Crystal structure of $K_{0.9}Mo_6O_{17}$ projected on the plane perpendicular to the a-axis (after Ref. (*12*)). Open and hatched circles indicate atomic positions at $y = 0$ and $\frac{1}{2}$, respectively.

The minimal O–O distance, which corresponds to the O(3)–O(9) edge in the NaO_{12} icosahedra, is 2.589(6) Å. The refinement of the occupancy factor of the sodium atom indicates the sodium concentration of 90%, which is consistent with the expected value from the sample preparation. Thus, the structure of $Na_{0.9}Mo_6O_{17}$ is found to be essentially similar to that of $K_{0.9}Mo_6O_{17}$. The slight difference between them may be due to the difference between the K^+ and Na^+ ion radii.

(*b*) *Estimation of the Molybdenum Valence*

In the molybdenum bronzes, the Mo–Mo distances are too large to form the metallic bonds due to the direct overlap of the 4*d*-wave function. Therefore the electronic properties should be discussed on the basis of the critical overlap integral between the molybdenum and oxygen atoms, namely, the Mo–O bond length. The two-dimensional slab structure with the ReO_3-type arrangement of the MoO_6 octahedra in $Na_{0.9}Mo_6O_{17}$ seems to explain the two-dimensionality of the electronic transport. Here, in order to make this respect more definite, we calculated the effective mean molybdenum valences, applying the bond length versus bond strength relation (*18*) to the obtained Mo–O bond lengths.

The results are listed in Table V and those obtained previously for $K_{0.9}Mo_6O_{17}$

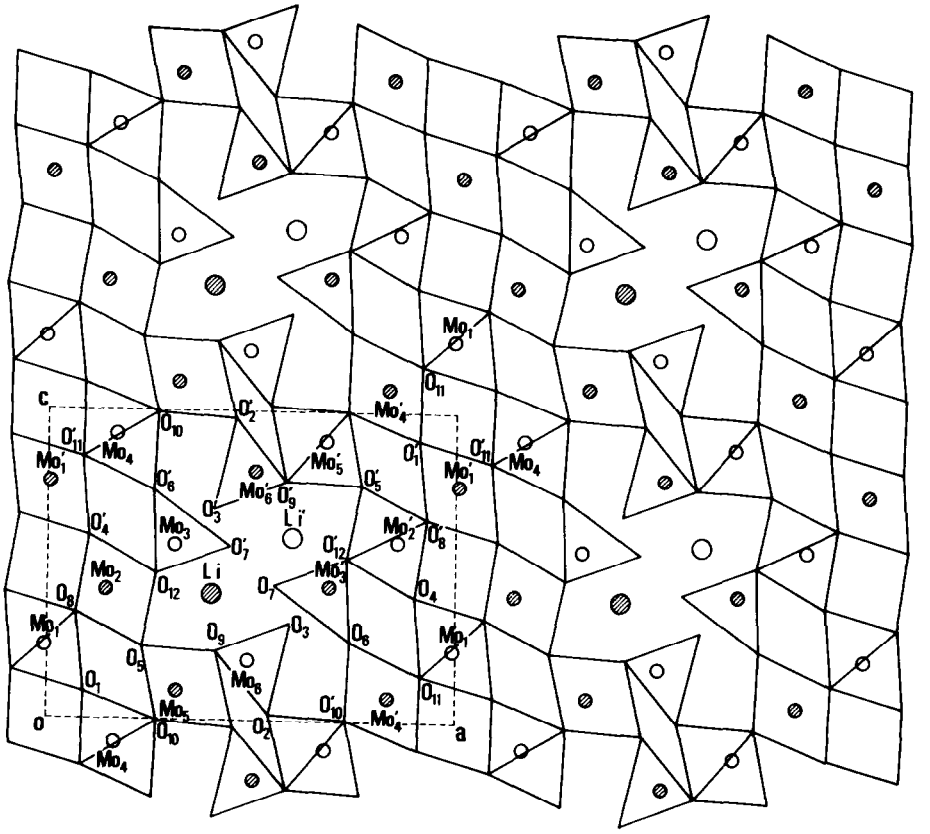

FIG. 3. Crystal structure of $Li_{0.9}Mo_6O_{17}$ projected on the *ac*-plane (after Ref. (*13*)). Open and hatched circles indicate atomic positions at $y = \frac{1}{4}$ and $\frac{3}{4}$, respectively.

(*12*) and $Li_{0.9}Mo_6O_{17}$ (*13*) are also listed. The conduction electron distribution in $Na_{0.9}Mo_6O_{17}$ is found to be very similar to that in $K_{0.9}Mo_6O_{17}$; the effective mean molybdenum valence for the MoO_4 site is 6.0+, indicating the absence of the conduction electron, and those for other MoO_6 sites are about 5.1+ and 5.7+. Thus, we can conclude that all of the 4*d*-electrons in $Na_{0.9}Mo_6O_{17}$ are located in the two-dimensional slabs of the MoO_6 octahedra, separated by the NaO_{12} icosahedra linked to the MoO_4 tetrahedra. It accounts successfully for the existence of the similar CDW transitions in $K_{0.9}Mo_6O_{17}$ (*7*, *8*) and $Na_{0.9}Mo_6O_{17}$ (*10*).

TABLE V

EFFECTIVE MEAN MOLYBDENUM VALENCES OF MOLYBDENUM PURPLE BRONZES

	$K_{0.9}Mo_6O_{17}$[a]	$Na_{0.9}Mo_6O_{17}$[b]	$Li_{0.9}Mo_6O_{17}$[c]
Mo(1)	6.0[d]	5.1	5.1
Mo(2)	5.1	5.7	5.7
Mo(3)	5.8	6.0[d]	5.8[d]
Mo(4)			5.0
Mo(5)			5.8
Mo(6)			5.8[d]

[a] Ref. (*12*).
[b] Present work.
[c] Ref. (*13*).
[d] MoO_4 tetrahedral site.

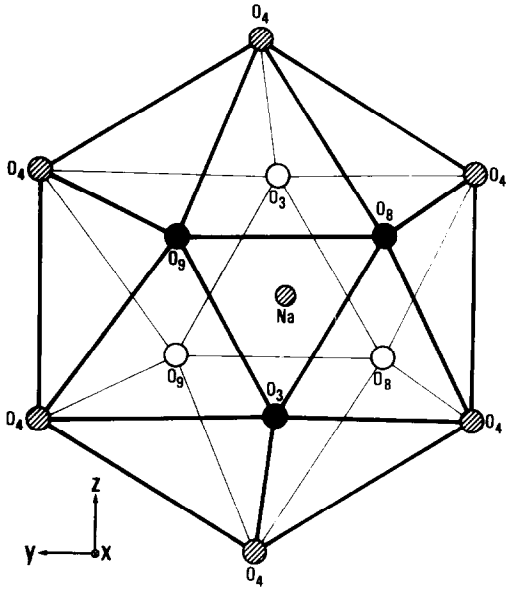

FIG. 4. The sodium atoms located in the oxygen icosahedron. Open, hatched, and solid circle indicate atomic positions at $x \simeq 0.66$, 0.5, and 0.34, respectively.

(c) *Structural Property and CDW Transition*

From the detailed crystal structures of $M_{0.9}Mo_6O_{17}$ shown in Figs. 1–3, we find that the compounds with the regular slabs of the pseudocubic linkage of the MoO_6 octahedra have the CDW states, while $Li_{0.9}Mo_6O_{17}$ with the rather distorted slabs does not undergo the CDW transition but becomes superconducting (*13, 19*). The difference between the CDW transition temperatures of $K_{0.9}Mo_6O_{17}$ and $Na_{0.9}Mo_6O_{17}$ is considered to be caused by the slight difference between their structures. It is quite reasonable to consider that the electronic properties in $M_{0.9}Mo_6O_{17}$ are mainly determined by the characteristics of the slabs. Therefore, it is interesting to compare the structural and the electronic properties of the molybdenum purple bronzes with those of the so-called Magnéli phase Mo_nO_{3n-1} ($n \geq 8$) which also have the similar slabs of the ReO_3-type linkage of the MoO_6 octahedra. For Mo_8O_{23}, Mo_9O_{26}, and $Mo_{10}O_{29}$, the superlattice reflections due to the CDW formation have been found at about 315, 500, and 610 K, respectively (*20*). The condensed modes are assigned to have characters similar to the M_3 mode of the ReO_3—type pseudocubic lattice, which are mainly described by rotations of the MoO_6 octahedra in the slabs with keeping the corner-linked structures. The transition temperature T_c increases with decreasing the average conduction electron number density n_e, which is simply estimated from their chemical formulae.

The superlattice points in the CDW states in $K_{0.9}Mo_6O_{17}$ (*8*) and $Na_{0.9}Mo_6O_{17}$ (*9, 10*) are easily known to correspond to the M points of the pseudocubic lattice of the slabs. We suppose their condensed modes have the same character as the case of Mo_nO_{3n-1}. $K_{0.9}Mo_6O_{17}$ and $Na_{0.9}Mo_6O_{17}$ have higher n_e and lower CDW transition temperatures T_c than those in Mo_nO_{3n-1}. Superconductivity appears when T_c becomes 0,

as is seen for $Li_{0.9}Mo_6O_{17}$. Therefore, $M_{0.9}Mo_6O_{17}$ and Mo_nO_{3n-1} may be the example series for the competition between the superconductivity and the CDW with changing the conduction electron number density, or possibly with changing the strength of the electron–phonon coupling in the slabs of the MoO_6 octahedra. To determine if this picture is correct, the mode assignments of the CDW states in $K_{0.9}Mo_6O_{17}$ and $Na_{0.9}Mo_6O_{17}$ are necessary.

Conclusion

In the present study, we have solved and refined the crystal structure of $Na_{0.9}Mo_6O_{17}$. The structure has been found to be essentially similar to that of $K_{0.9}Mo_6O_{17}$, although their space groups are different. It has been shown that both the structure and the conduction electron distribution in $Na_{0.9}Mo_6O_{17}$ lead to the two-dimensional electronic transport. The existence of the similar CDW transitions in $K_{0.9}Mo_6O_{17}$ and $Na_{0.9}Mo_6O_{17}$ can be well understood by their structural properties.

It is suggested that $Na_{0.9}Mo_6O_{17}$ is one of the compound series with the slabs of the pseudocubic linkage of the MoO_6 octahedra which shows the possible competition between the superconductivity and the CDW with changing the electron number density, or with the resulting change of the electron–phonon coupling.

Acknowledgment

The authors sincerely thank Dr. K. Toriumi for his valuable suggestion with respect to the absorption correction.

References

1. For example, see M. SATO, B. H. GRIER, H. FUJISHITA, S. HOSHINO, AND A. R. MOODENBAUGH, *J. Phys. C* **16,** 527 (1983).
2. H. NAGASAWA, T. ERATA, M. ONODA, H. SUZUKI, S. UJI, Y. KANAI, AND S. KAGOSHIMA, *Mol. Cryst. Liq. Cryst.* **121,** 121 (1985), and references therein.
3. For example, see "Proceedings, International Conference on Charge Density Waves in Solids, Budapest, 1984" (G. Hutiray and J. Sólyom, Eds.), Springer-Verlag, Berlin (1985).
4. A. WOLD, W. KUNNMANN, R. J. ARNOTT, AND A. FERRETI, *Inorg. Chem.* **3,** 535 (1964).
5. J-M. RÉAU, C. FOUASSIER, AND P. HAGENMULLER, *J. Solid State Chem.* **1,** 326 (1970).
6. W. H. MCCARROLL AND M. GREENBLATT, *J. Solid State Chem.* **54,** 282 (1984).
7. R. BUDER, J. DEVENYI, J. DUMAS, J. MARCUS, J. MARCIER, C. SCHLENKER, AND H. VINCENT, *J. Phys. Lett. (Orsay, Fr.)* **43,** 59 (1982).
8. C. ESCRIBE-FILIPPINI, R. ALMAIRAC, R. AYROLES, C. ROUCAU, K. KONATÉ, J. MARCUS, AND C. SCHLENKER, *Philos. Mag. B* **50,** 321 (1984).
9. C. SCHLENKER, J. DUMAS, C. ESCRIBE-FILIPPINI, H. GUYOT, J. MARCUS, AND G. FOURCAUDOT, *Philos. Mag. B* **52,** 643 (1985).
10. C. ESCRIBE-FILIPPINI, J. MARCUS, C. SCHLENKER, R. AYROLES, S. KAGOSHIMA, AND J. P. POUGET, to be published.
11. M. GREENBLATT, W. H. MCCARROLL, R. NEIFELD, M. CROFT, AND J. V. WASZCZAK, *Solid State Commun.* **51,** 671 (1984).
12. H. VINCENT, M. GHERDIRA, J. MARCUS, J. MERCIER, AND C. SCHLENKER, *J. Solid State Chem.* **47,** 113 (1983).
13. M. ONODA, K. TORIUMI, Y. MATSUDA, AND M. SATO, *J. Solid State Chem.* **66,** 163 (1987).
14. N. C. STEPHENSON, *Acta Crystallogr.* **20,** 59 (1966).
15. T. SAKURAI AND K. KOBAYASHI, *Rikagaku Kenkyusho Hokoku* **55,** 69 (1979). [in Japanese]
16. P. COPPENS, T. N. GURU ROW, P. LEUNG, E. D. STEVENS, P. J. BECKER, AND Y. W. YANG, *Acta Crystallogr., Sect. A* **35,** 63 (1979).
17. "International Tables for X-Ray Crystallography" (J. A. Ibers and W. C. Hamilton, Eds.), Vol. IV, Kynoch Press, Birmingham, England (1974).
18. W. H. ZACHARIASEN, *J. Less-Common Met.* **62,** 1 (1978).
19. Y. MATSUDA, M. SATO, M. ONODA, AND K. NAKAO, *J. Phys. C* **19,** 6039 (1986).
20. M. ONODA, H. FUJISHITA, Y. MATSUDA, AND M. SATO, *Synth. Met.* **19,** 947 (1987).